*condensed matter*

MDPI

*Article*

# Magnetic Evolution of Carrier Doping and Spin Dynamics in Diluted Magnetic Semiconductors (Ba,Na)(Zn,Mn)$_2$As$_2$

**Guoqiang Zhao [1,2,3,*], Yipeng Cai [3,4], Kenji M. Kojima [4], Qi Sheng [3], James Beare [5], Graeme Luke [4,5], Xiang Li [1], Yi Peng [2], Timothy Ziman [1], Kan Zhao [2], Zheng Deng [2,6], Xiancheng Wang [2,6], Yongqing Li [2,6], Gang Su [1,7], Sadamichi Maekawa [1,8,9], Bo Gu [1,*], Yasutomo J. Uemura [3,*] and Changqing Jin [2,6,*]**

1 Kavli Institute for Theoretical Sciences, University of Chinese Academy of Sciences, Beijing 101408, China; lixiang21@mails.ucas.ac.cn (X.L.); ziman@ill.fr (T.Z.); gsu@ucas.ac.cn or sugang@itp.ac.cn (G.S.); sadamichi.maekawa@riken.jp or sadamichimaekawa@gmail.com (S.M.)
2 Beijing National Laboratory for Condensed Matter Physics, Institute of Physics, Chinese Academy of Sciences, Beijing 100190, China; ypeng@iphy.ac.cn (Y.P.); zhaokan1986@163.com (K.Z.); dengzheng@iphy.ac.cn (Z.D.); wangxiancheng@iphy.ac.cn (X.W.); yqli@iphy.ac.cn (Y.L.)
3 Department of Physics, Columbia University, New York, NY 10027, USA; caidia52@gmail.com (Y.C.); q_sheng@outlook.com (Q.S.)
4 TRIUMF, Vancouver, BC V6T 2A3, Canada; kojima@triumf.ca (K.M.K.); luke@mcmaster.ca (G.L.)
5 Department of Physics and Astronomy, McMaster University, Hamilton, ON L8S 4M1, Canada; bearej@mcmaster.ca
6 School of Physics, University of Chinese Academy of Sciences, Beijing 101408, China
7 Institute of Theoretical Physics, Chinese Academy of Sciences, Beijing 100190, China
8 RIKEN Center for Emergent Matter Science (CEMS), Wako 315-0198, Japan
9 Advanced Science Research Center (ASRC), Japan Atomic Energy Agency, Tokai 319-1195, Japan
* Correspondence: g.q.zhao@iphy.ac.cn (G.Z.); gubo@ucas.ac.cn (B.G.); yu2@columbia.edu (Y.J.U.); jin@iphy.ac.cn (C.J.)

**Abstract:** The investigation of novel diluted magnetic semiconductors (DMSs) provides a promising platform for studying magnetism and transport characteristics, with significant implications for spintronics. DMSs based on $BaZn_2As_2$ are particularly noteworthy due to their high Curie temperature ($T_C$) of 260 K, diverse magnetic states, and potential for multilayer heterojunctions. This study investigates the magnetic evolution of carrier doping and spin dynamics in the asperomagnet (Ba,Na)(Zn,Mn)$_2$As$_2$, utilizing a combination of magnetization measurements, ac susceptibility, and muon spin rotation (μSR). Key findings include the following: (1) lower transition temperatures and coercive forces in (Ba,Na)(Zn,Mn)$_2$As$_2$ compared to the ferromagnet (Ba,K)(Zn,Mn)$_2$As$_2$; (2) a dynamic fluctuation peak around the transition temperature observed in both the ac susceptibility and longitudinal field (LF) μSR; and (3) the coexistence of static and dynamic states at low temperatures, exhibiting spin-glass-like characteristics. This study, to the best of our knowledge, may represent the first investigation of asperomagnetic order utilizing μSR techniques. It enhances the understanding of magnetic interactions in $BaZn_2As_2$-based systems and provides valuable insights into the exploration of high $T_C$ DMSs.

**Keywords:** diluted magnetic semiconductor; magnetic evolution; dynamic fluctuation



Academic Editors: Charles H. Mielke and Amir-Abbas Haghighirad

Received: 27 March 2025
Revised: 12 May 2025
Accepted: 13 May 2025
Published: 15 May 2025

**Citation:** Zhao, G.; Cai, Y.; Kojima, K.M.; Sheng, Q.; Beare, J.; Luke, G.; Li, X.; Peng, Y.; Ziman, T.; Zhao, K.; et al. Magnetic Evolution of Carrier Doping and Spin Dynamics in Diluted Magnetic Semiconductors (Ba,Na)(Zn,Mn)$_2$As$_2$. *Condens. Matter* **2025**, *10*, 30. https://doi.org/10.3390/condmat10020030



## 1. Introduction

Diluted magnetic semiconductors (DMSs) [1–4] are of great research interest for their exceptional properties and potential in spintronic devices [5,6]. Studying new DMSs with high Curie temperature ($T_C$) and versatile magnetic states offers valuable insights into the interactions between magnetism and transport properties [7]. Manganese (Mn)-doped

II-VI [2] and III-V DMSs [3,6,8], such as (Ga,Mn)As, have been extensively researched since their discovery [9,10]. However, $T_C$ is still far from room temperature, and the underlying mechanisms of magnetic exchange interactions continue to be a matter of ongoing debate [8,11]. In 2007, Masek, Jungwirth, and their colleagues introduced a new generation of DMSs featuring independent spin and charge doping mechanisms, such as Li(Zn,Mn)As [12], which was synthesized shortly thereafter [13]. Unlike (Ga,Mn)As, where $Ga^{3+}/Mn^{2+}$ substitutions provide both charge carriers and spin simultaneously, the Li(Zn, Mn)As allows for independent control of charge (e.g., excess $Li^{1+}$) and spin (e.g., $Zn^{2+}/Mn^{2+}$). Li(Zn,Mn)As is isostructural to (Ga,Mn)As, and its study may offer valuable insights into magnetic interactions and magnetic orderings in DMSs. Consequently, a novel wave of experimental research has emerged since 2011 [4], concentrating on the development of a series of Mn-based DMS systems characterized by independent spin and charge doping [1,14–67]. Among them, DMSs based on $BaZn_2As_2$ have emerged as a prominent material system due to their high $T_C$ of 260 K [65], diverse magnetic states [1,21,44], and potential for multilayer heterojunctions [68]. Despite the advantages mentioned above, the understanding of the nature of magnetic interactions in DMSs based on $BaZn_2As_2$ is still far from perfect. $(Ba,K)(Zn,Mn)_2As_2$ (BKZMA) shows ferromagnetic (FM) properties, whereas $(Ba,Na)(Zn,Mn)_2As_2$ (BNZMA) exhibits an asperomagnetic order [1], an intermediate regime between an FM and a canonical spin glass (SG). Asperomagnets can be considered variants of SG. Their essential feature is that some random frustration of the exchange interactions leads to many nearly degenerate ground states. Furthermore, the reduced FM order observed in BKZMA can be ascribed to the influence of chemical pressure [40–42]. In contrast, the diminished FM order in BNZMA is attributed to an increased concentration of hole carriers [1], which can enhance the antiferromagnetic portion of the oscillatory Ruderman–Kittel–Kasuya–Yosida (RKKY) interactions [69,70]. To enhance the understanding of magnetic interactions in BNZMA, this study focuses on the study of the magnetic evolution of carrier doping and spin dynamics by utilizing a combination of magnetization measurements, ac susceptibility, and muon spin rotation (μSR). Following this introductory chapter, we will present the magnetic evolution of carrier doping and spin dynamics, along with a comparison to previously reported findings in BKZMA [21,65], all in the results section. The main results and potential directions for further research will be elucidated in the discussion and concluding section, which follows a brief explanation of the materials and methods employed.

## 2. Results

### *2.1. Structural Characterization*

The parent compound β-$BaZn_2As_2$ crystallizes in the $ThCr_2Si_2$-type structure, characterized by the space group I4/mmm [21]. Similar to BKZMA, BNZMA also displays the same structural characteristics, as shown in Figure 1b. The X-ray diffraction (XRD) patterns, presented in Figure 1a, along with the refined data obtained from the powder specimen of $(Ba_{0.9}Na_{0.1})(Zn_{0.85}Mn_{0.15})_2As_2$, were analyzed using Rietveld refinement and can be accurately indexed to a single phase. The resultant weighted reliability factor ($R_{wp}$) is approximately 3.40%. As the doping levels of sodium (Na) increase, a monotonic decrease is observed in the a-axis, c-axis, and volume, as illustrated in Figure 2b. This observation indicates successful doping, as the ionic radius of $Na^{1+}$ (1.02 Å) is smaller than that of $Ba^{2+}$ (1.35 Å), both with coordination numbers of six.

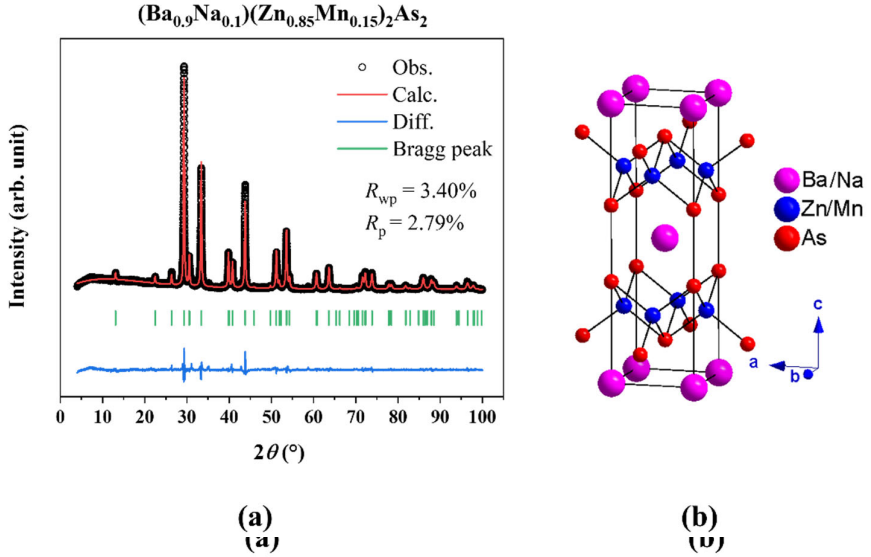


**Figure 1.** (**a**) X-ray diffraction (XRD) pattern of the powder sample $(Ba_{0.9}Na_{0.1})(Zn_{0.85}Mn_{0.15})_2As_2$, accompanied by Rietveld analysis, (**b**) The crystal structure of $(Ba,Na)(Zn,Mn)_2As_2$.

**Figure 1.** (**a**) X-ray diffraction (XRD) pattern of the powder sample $(Ba_{0.9}Na_{0.1})(Zn_{0.85}Mn_{0.15})_2As_2$, accompanied by Rietveld analysis, (**b**) The crystal structure of $(Ba,Na)(Zn,Mn)_2As_2$.

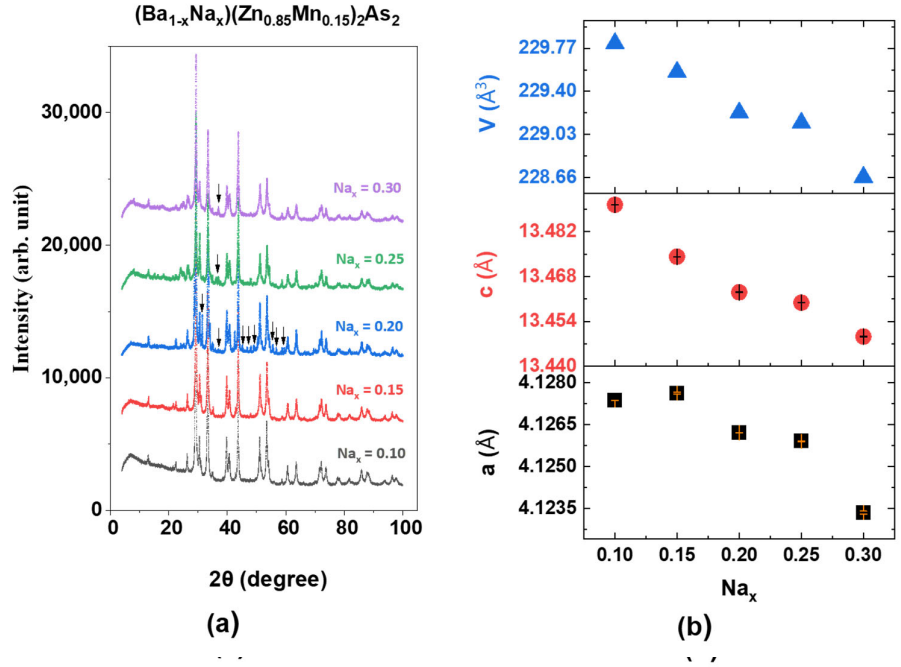


**Figure 2.** (**a**) XRD pattern of the powder sample $(Ba_{1-x}Na_x)(Zn_{0.85}Mn_{0.15})_2As_2$ (where x = 0.10, 0.15, 0.20, 0.25, and 0.30). The black arrow indicates the low-temperature $BaZn_2As_2$-based phase, which belongs to the space group *P*-3*m*1 [27]. (**b**) Lattice constants and cell volumes of the samples. The error bar of the a and c parameters were also indicated.

**Figure 2.** (**a**) XRD pattern of the powder sample $(Ba_{1-x}Na_x)(Zn_{0.85}Mn_{0.15})_2As_2$ (where x = 0.10, 0.15, 0.20, 0.25, and 0.30). The black arrow indicates the low-temperature $BaZn_2As_2$-based phase, which belongs to the space group *P*-3*m*1 [27]. (**b**) Lattice constants and cell volumes of the samples. The error bar of the a and c parameters were also indicated.

### 2.2. Magnetization and Magnetic Critical Behaviors

Under an external magnetic field of 500 Gauss (G), the magnetic susceptibility $\chi_{ZFC}(T)$ (measured in zero field cooling (ZFC) mode) and $\chi_{FC}(T)$ (measured in field cooling (FC) mode) of all these $(Ba_{1-x}Na_x)(Zn_{0.85}Mn_{0.15})_2As_2$ samples (where x = 0.10, 0.15, 0.20, 0.25, and 0.30) are shown in Figure 3a and Figure 3b, respectively. Three key findings can be clearly seen. (1) As illustrated in Figure 4, prior research indicates that BKZMA is a ferromagnet [21], whereas BNZMA exhibits an asperomagnetic order at 12 K (8 K) in the fields parallel (perpendicular) to the c-axis [1]. To enable a direct comparative analysis, we adopted the Curie–Weiss law to investigate the magnetic interactions within the compound $(Ba_{1-x}X_x)(Zn_{0.85}Mn_{0.15})_2As_2$, where X denotes Na and potassium (K).

### 2.2. Magnetization and Magnetic Critical Behaviors

Under an external magnetic field of 500 Gauss (G), the magnetic susceptibility $\chi_{ZFC}(T)$ (measured in zero field cooling (ZFC) mode) and $\chi_{FC}(T)$ (measured in field cooling (FC) mode) of all these $(Ba_{1-x}Na_x)(Zn_{0.85}Mn_{0.15})_2As_2$ samples (where x = 0.10, 0.15, 0.20, 0.25, and 0.30) are shown in Figure 3a and Figure 3b, respectively. Three key findings can be clearly seen. (1) As illustrated in Figure 4, prior research indicates that BKZMA is a ferromagnet [21], whereas BNZMA exhibits an asperomagnetic order at 12 K (8 K) in the fields parallel (perpendicular) to the c-axis [1]. To enable a direct comparative analysis, we adopted the Curie–Weiss law to investigate the magnetic interactions within the compound $(Ba_{1-x}X_x)(Zn_{0.85}Mn_{0.15})_2As_2$, where X denotes Na and potassium (K).

(perpendicular) to the c-axis [1]. To enable a direct comparative analysis, we adopted the Curie–Weiss law to investigate the magnetic interactions within the compound $(Ba_{1-x}X_x)(Zn_{0.85}Mn_{0.15})_2As_2$, where X denotes Na and potassium (K). With a nominal hole carrier doping level (via Ba/K or Ba/Na substitution) ranging from 10% to 30%, the transition temperature in BKZMA varies from 40 K to 190 K [21], whereas in BNZMA, it only ranges from 38.5 K to 72.7 K. This disparity suggests that the crystal structure distortion plays a significant role in influencing magnetic interactions, particularly given that both compounds exhibit similar hole carrier doping levels with equivalent Ba/K or Ba/Na substitutions. This observation was also in accordance with the physical pressure study conducted on BKZMA [42]. The susceptibility values in BNZMA are approximately one order of magnitude smaller than those in BKZMA [21], which is consistent with previous studies on the single crystal $(Ba_{0.907}Na_{0.093})(Zn_{0.819}Mn_{0.181})_2As_2$ [1]. Furthermore, as illustrated in Figure 3b, the coercive fields for BNZMA are only in the range of several hundred Gauss (G), indicating that it exhibits soft magnetic properties, in contrast to the hard magnetic characteristics of BKZMA [21,27,65]. (3) In both the polycrystalline and single-crystalline samples, the zero-field-cooled (ZFC) magnetization demonstrated a notable divergence from the field-cooled (FC) magnetization below a particular temperature for both BKZMA [21,27,65] and BNZMA [1]. This phenomenon cannot be ascribed to magnetic anisotropy because a variety of material systems with polycrystalline states demonstrate this characteristic, including Li(Zn,Cu,Mn)As [39], Na(Zn,Mn)Sb [64], $Ba(Zn,Cu,Mn)_2As_2$ [29], $(Ba,K)(Cu,Mn)_2Se_2$ [37], (Ba,Na)F(Zn,Mn)Sb [63], SrF(Zn,Mn,Cu)Sb [48], and (La,X)(Zn,Mn)AsO [15,17,23,35,62], where X denotes Ca, Sr, or Ba. The bifurcation point is referred to as the spin freezing temperature, $T_f$. ac susceptibility measurements of the single crystal $(Ba_{0.907}Na_{0.093})(Zn_{0.819}Mn_{0.181})_2As_2$ have indicated a spin-glass-like characteristic [1]. Nevertheless, the material does not display the characteristic behavior of a canonical SG, as evidenced by the continuous increase in $\chi'$ with decreasing temperature. To explore this further, we investigated the dynamic magnetic properties near $T_f$ of BNZMA at different doping levels and employed both ac susceptibility and longitudinal field (LF) μSR techniques, as detailed in the following sections.

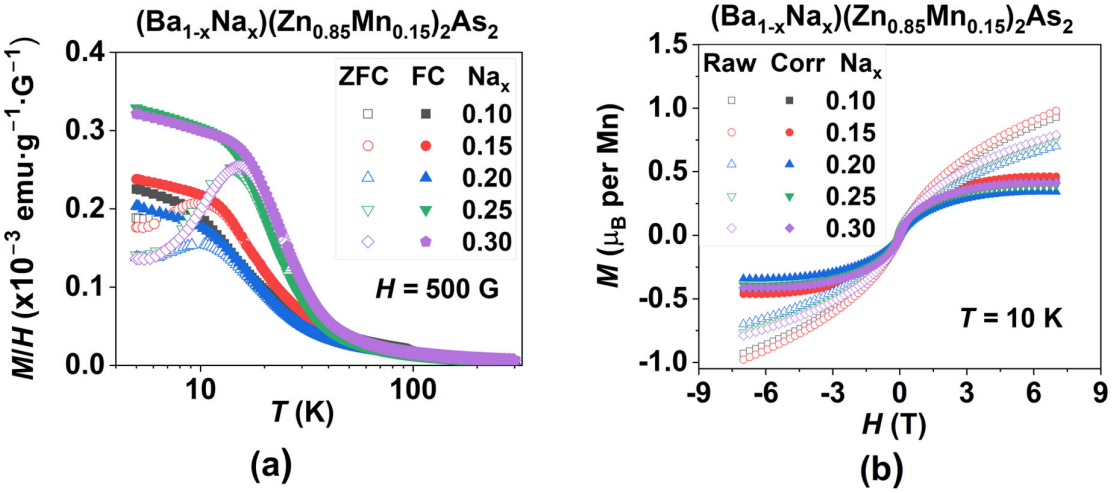


**Figure 3.** The effect of carrier doping on the magnetization of $(Ba_{1-x}Na_x)(Zn_{0.85}Mn_{0.15})_2As_2$ (where x = 0.10, 0.15, 0.20, 0.25, and 0.30). (**a**) The direct current (dc) magnetization was measured at a magnetic field of $H$ = 500 Gauss (G). (**b**) The magnetic hysteresis curve $M(H)$ was obtained through field training, along with the subtraction of the paramagnetic component, measured at a temperature of $T$ = 2 K.

The ac susceptibility can serve as a valuable probe for investigating magnetic dynamics within the low-frequency regime, characterized by correlation times that span from approximately 1 s to $10^{-5}$ s [71]. As a complementary technique, magnetic resonance is utilized in conjunction with μSR over time scales ranging from approximately $10^{-6}$ s

to $10^{-12}$ s [72,73]. By integrating these two methods, it is possible to ascertain the correlation time or fluctuation rate over an extensive range [74]. As illustrated in Figure 5, a distinct peak is evident around $T_f$ in both the real and imaginary components of the $(Ba_{0.75}Mn_{0.25})(Zn_{0.85}Mn_{0.15})_2As_2$ polycrystalline samples, while the position of the peak varies with frequency. Figure 6a shows the LF μSR time spectra at various selected temperatures. The analysis was conducted using the following function over a time range of one to eight microseconds, with a packing number of ten:

$$Asymmetry(t) = Asy_{temp.} exp\left[-\left(\frac{t}{T_1}\right)^{\beta}\right] (0.5 < \beta < 1)$$



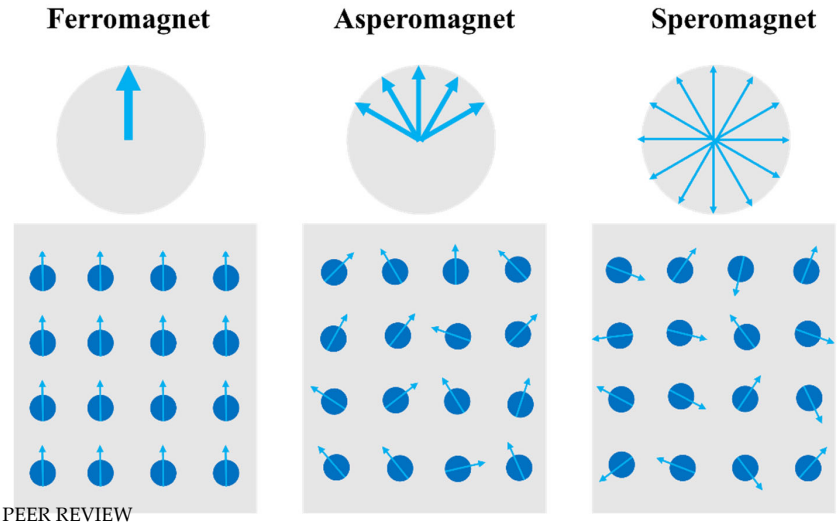




**Figure 4.** Schematic illustration of the ferromagnet, asperomagnet, and speromagnet.

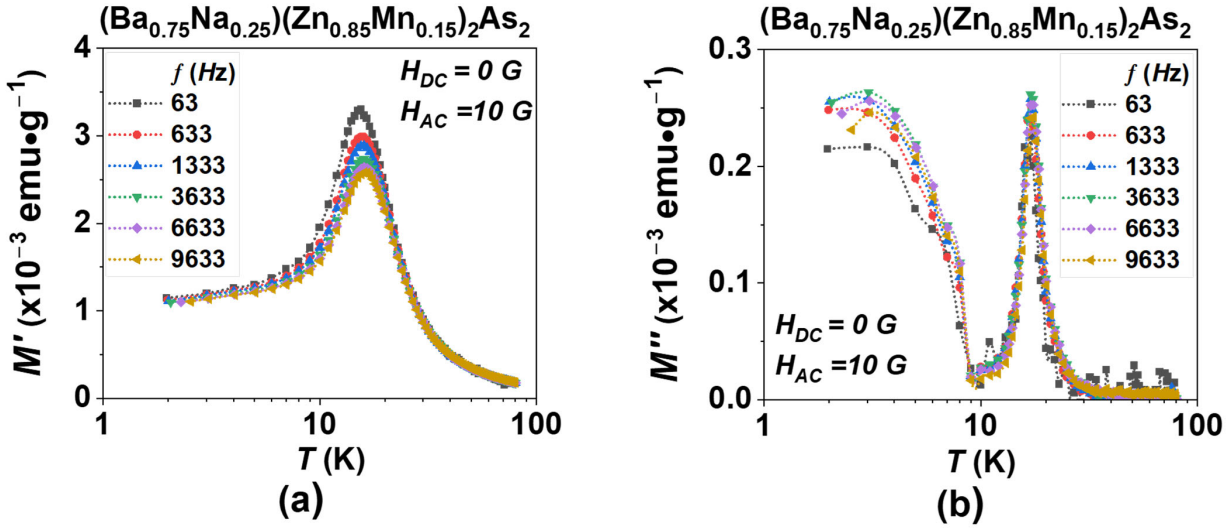


**Figure 5.** ac susceptibility results of the polycrystalline specimen $(Ba_{0.75}Na_{0.25})(Zn_{0.85}Mn_{0.15})_2As_2$: (**a**) real part; (**b**) imaginary part.

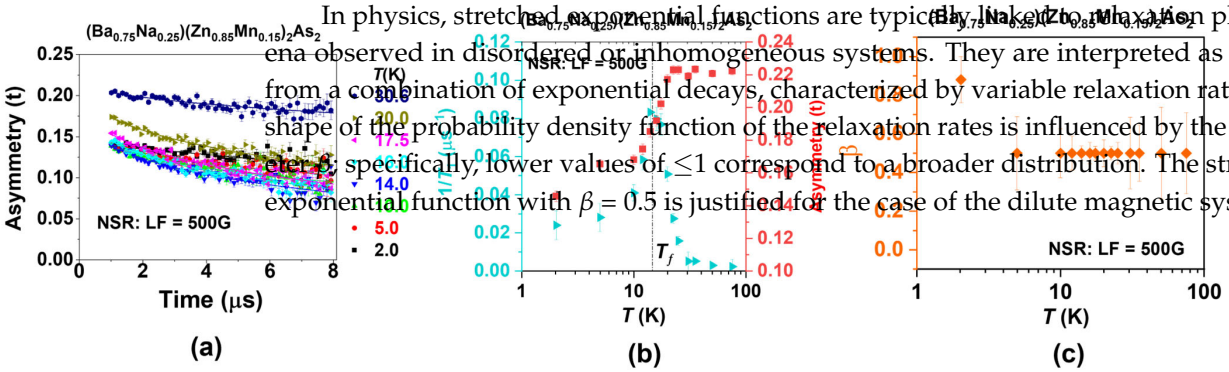


shape of the probability density function of the relaxation rates is influenced by the parameter $\beta$; specifically, lower values of $\leq 1$ correspond to a broader distribution. The stretched exponential function with $\beta = 0.5$ is justified for the case of the dilute magnetic

In physics, stretched exponential functions are typically linked to relaxation phenomena observed in disordered or inhomogeneous systems. They are interpreted as arising from a combination of exponential decays, characterized by variable relaxation rates. The shape of the probability density function of the relaxation rates is influenced by the parameter $\beta$; specifically, lower values of $\leq 1$ correspond to a broader distribution. The stretched exponential function with $\beta = 0.5$ is justified for the case of the dilute magnetic system in

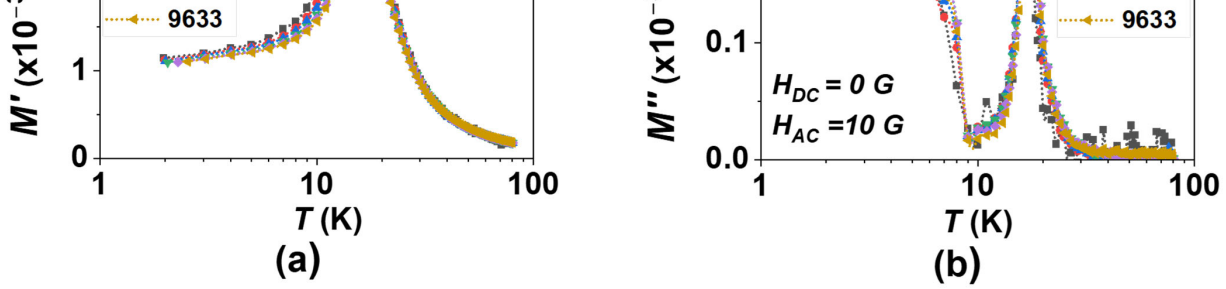


**Figure 5.** ac susceptibility results of the polycrystalline specimen $(Ba_{0.75}Na_{0.25})(Zn_{0.85}Mn_{0.15})_2As_2$: (**a**) real part, (**b**) imaginary part.

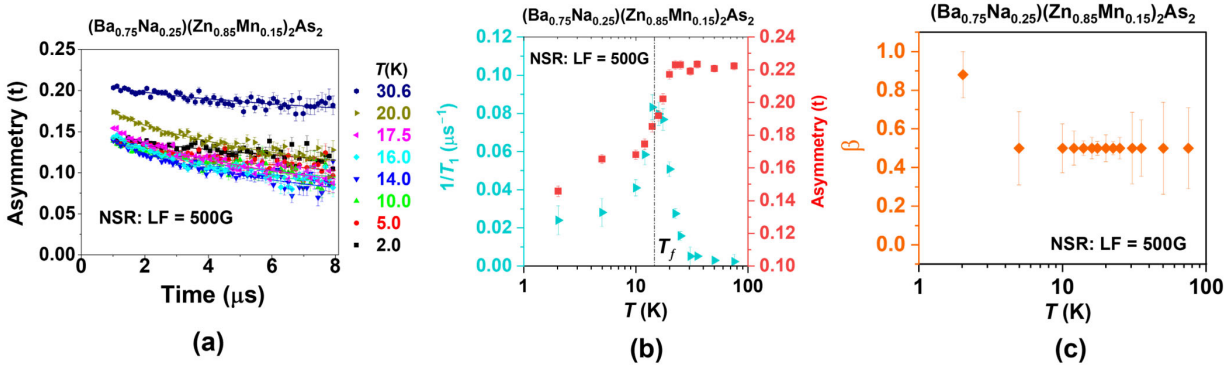


**Figure 6.** (**a**) μSR time spectra of $(Ba_{0.75}Mn_{0.25})(Zn_{0.85}Mn_{0.15})_2As_2$ with a polycrystalline sample under longitudinal field configuration. (**b**) $1/T_1$ and asymmetry as a function of temperature. (**c**) Stretched exponential parameter as a function of temperature.

### 2.3. Magnetic Ground State

The magnetic ground state and spin dynamics can be investigated through longitudinal LF μSR measurements at a base temperature [72,73]. The presence of static magnetism suggests that when an external magnetic field is applied parallel to the initial direction of the muon spin, it decouples the spectral line shape (Asymmetry(t)) from the internal magnetic fields. When the external fields are approximately ten times greater than the internal fields, Asymmetry(t) stabilizes and becomes constant over time. However, in a dynamic magnetic system (Figure 3 in reference [76]), this decoupling is not achievable for small fields, resulting in Asymmetry(t) remaining largely unaffected by the external field. As shown in Figure 7, when the field reaches 1 kG, which is about ten times larger than the coercive force in $(Ba_{0.75}Na_{0.25})(Zn_{0.85}Mn_{0.15})_2As_2$ polycrystalline specimen, there exists a coexistence of the static and dynamic magnetism. This feature is also noted in the SG CuMn alloy (Figure 9 in reference [75]).



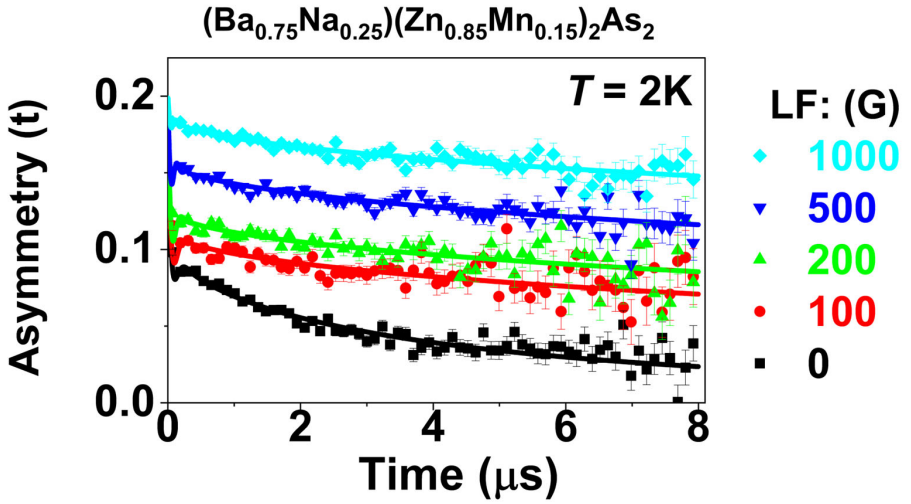


**Figure 7.** Longitudinal field (LF) μSR spectra were obtained at a base temperature of 2K for the polycrystalline specimen of $(Ba_{1-x}Na_x)(Zn_{0.85}Mn_{0.15})_2As_2$.

## 3. Materials and Methods

Polycrystalline specimens of $(Ba_{1-x}Na_x)(Zn_{0.85}Mn_{0.15})_2As_2$ (where x = 0.10, 0.15, 0.20, 0.25, and 0.30) were synthesized using a solid-state reaction method with high-purity reagents [13]. The precursor materials, BaAs and $Na_3As$, were sintered at 500 °C and 200 °C for 40 h in a sealed titanium tube with high-purity Ba, Na, and As. These precursors, along

## 3. Materials and Methods

Polycrystalline specimens of $(Ba_{1-x}Na_x)(Zn_{0.85}Mn_{0.15})_2As_2$ (where x = 0.10, 0.15, 0.20, 0.25, and 0.30) were synthesized using a solid-state reaction method with high-purity reagents [13]. The precursor materials, BaAs and $Na_3As$, were sintered at 500 °C and 200 °C for 40 h in a sealed titanium tube with high-purity Ba, Na, and As. These precursors, along with Zn, Mn, and As powders, were loaded into a titanium tube with the nominal composition of $(Ba,Na)(Zn,Mn)_2As_2$ under an argon atmosphere at 1 atm pressure then placed in a quartz tube. The mixtures were heated to 750 °C for 30 h and cooled to room temperature at 2 °C/min. Specimens were analyzed using X-ray powder diffraction with a Philips X'pert diffractometer and CuK$\alpha$-radiation. Direct current (dc) magnetic susceptibility was measured with a superconducting quantum interference device (SQUID) magnetometer, while alternating current (ac) magnetic susceptibility measurements were conducted on a physical property measurement system (PPMS). Positive muon spin relaxation ($\mu$SR) measurements were performed on polycrystalline specimens of $(Ba_{0.75}Na_{0.25})(Zn_{0.85}Mn_{0.15})_2As_2$ at the Center for Molecular and Materials Sciences at TRIUMF in Vancouver, Canada.

## 4. Discussion and Conclusions

Asperomagnets and speromagnets are differentiated by the length scale at which spin correlations average to zero. In the case of speromagnets, this occurs over, at most, a few interatomic spacings, characterized by antiferromagnetic nearest-neighbor correlations. Conversely, in asperomagnets, the length scale is significantly greater, resulting in integrated correlations that exhibit ferromagnetic behavior on a mesoscopic scale [77]. Compared to ferromagnets, asperomagnets exhibit ferromagnetic hysteresis with notable remanence ($M_r$) at low temperatures. The ratio of remanence to saturation moment ($M_r$ / $M_s$) ranges from 0.1 to 0.5 [78]. In the representative material DyCu, this value is 0.26 [79]. When roughly comparing the value between the asperomagnet $(Ba_{0.8}Na_{0.2})(Zn_{0.85}Mn_{0.15})_2As_2$ (Figure 3b; $M_r$ = 0.34) and ferromagnet $(Ba_{0.8}K_{0.2})(Zn_{0.90}Mn_{0.10})_2As_2$ (Figure 2b in reference [21]; $M_s$ = 1.10), this value is approximately 0.31.

In addition to the impact of the higher hole concentrations [1], several factors may contribute to the asperomagnetic behavior observed in BNZMA, including complex magnetic coupling and disorder. This is because the ionic radius of $Na^{1+}$ (1.02 Å) is much smaller than that of $Ba^{2+}$ (1.35 Å), which may cause the possibility of structural defects, such as interstitial $Na^{1+}$ ions, disorder, or compositional inhomogeneities. Previous studies have demonstrated the relationship between structure and magnetism by confirming the superstructures in the Li(Zn,Mn)As system [53]. Moreover, the replacement of Ba/Na could be viewed as a chemical pressure, which also tunes the magnetic coupling. This could be further supported by the physical pressure experiments on BKZMA [40–42]. Consequently, further exploration through more comprehensive studies, particularly on single crystals with fewer defects, is still needed. Such studies should integrate various techniques, including, but not limited to, scanning transmission electron microscopy (STEM), scanning tunneling microscopy (STM), and angle-resolved photoemission spectroscopy (ARPES), alongside theoretical calculations.

In summary, a systematic investigation of magnetic evolution, carrier doping, and spin dynamics has been conducted on the asperomagnet BNZMA. This compound exhibits significant differences when compared to its counterpart BKZMA and canonical SG. These observations yield two interesting insights: first, the presence of complex magnetic interactions within this system; and second, the magnetic evolution in response to temperature, chemical pressure, and doping levels. This information will be invaluable for

materials scientists aiming to discover higher $T_C$ or even room-temperature DMSs beyond the $BaZn_2As_2$ system in the future.

**Author Contributions:** This project was conceived by G.Z. in consultation with Y.J.U., C.J., B.G.; G.Z., and C.J. synthesized these materials, aided by useful discussions with Y.P., K.Z., Z.D., X.W.; G.Z., and Y.P. conducted the XRD pattern measurements and Rietveld refinement analysis; G.Z. and C.J. conducted dc magnetization, while G.Z. conducted the ac susceptibility measurements; The μSR data were collected by G.Z., Y.C., K.M.K., Q.S., J.B., G.L., and Y.J.U. and analyzed by G.Z., Y.J.U.; B.G., X.L., Y.L., S.M., and G.S. G.Z. offered useful discussions of the magnetic data; G.Z. generated a draft of the manuscript, assisted by valuable discussions with T.Z., which was then circulated to all the authors for their revisions and approval. All authors have read and agreed to the published version of the manuscript.

**Funding:** This project was financially supported by National Key Research and Development Projects of China (Grant Nos. 2022YFA1405100 and 2022YFA1204100), the National Natural Science Foundation of China (Grants Nos. 12074378 and 61888102), and the Chinese Academy of Sciences (Grant Nos. YSBR-030, JZHKYPT-2021-08, and XDB33000000). SM is supported by JSPS KAKENHI grant No. JP24K00576. G. Q. Zhao has received partial support from the China Scholarship Council (No. 201904910900), the Plan of Assistant to Special Researcher at the University of Chinese Academy of Sciences (2022-PASR-202206), and the CAS Project for Young Scientists in Basic Research (2022YSBR-048). The work at Columbia was supported by US National Science Foundation with the grant DMR 2104661.

**Data Availability Statement:** Raw μSR data are available in the TRIUMF. For further details, pleaserefer to the website: https://musr.ca/mud/runSel.html (accessed on 28 November 2019.).

**Acknowledgments:** We thank all the collaborators of the earlier (Ba,Na)(Zn,Mn)2As2 paper (doi: 10.1063/1.5010988). We thank Youwen Long and Shijun Qin for their support with the ac susceptibility measurements.

**Conflicts of Interest:** The authors declare no conflicts of interest.

## References

1. Gu, G.; Zhao, G.; Lin, C.; Li, Y.; Jin, C.; Xiang, G. Asperomagnetic order in diluted magnetic semiconductor (Ba,Na)$(Zn,Mn)_2As_2$. *Appl. Phys. Lett.* **2018**, *112*, 032402. [CrossRef]
2. Furdyna, J.K. Diluted magnetic semiconductors. *J. Appl. Phys.* **1988**, *64*, R29. [CrossRef]
3. Dietl, T.; Ohno, H. Dilute ferromagnetic semiconductors: Physics and spintronic structures. *Rev. Mod. Phys.* **2014**, *86*, 187–251. [CrossRef]
4. Zhao, G.; Deng, Z.; Jin, C. Advances in new generation diluted magnetic semiconductors with independent spin and charge doping. *J. Semicond.* **2019**, *80*, 081505. [CrossRef]
5. Žutić, I.; Fabian, J.; Sarma, S.D. Spintronics Fundamentals and applications. *Rev. Mod. Phys.* **2004**, *76*, 323.
6. Jungwirth, T.; Wunderlich, J.; Novák, V.; Olejník, K.; Olejník, K.; Gallagher, B.L.; Campion, R.P.; Edmonds, K.W. Spin-dependent phenomena and device concepts explored in (Ga,Mn)As. *Rev. Mod. Phys.* **2014**, *86*, 855–896. [CrossRef]
7. Dietl, T.; Bonanni, A.; Ohno, H. Families of magnetic semiconductors—An overview. *J. Semicond.* **2019**, *40*, 080301. [CrossRef]
8. Jungwirth, T.; Sinova, J.; Mašek, J.; Kučera, J.; MacDonald, A.H. Theory of ferromagnetic (III,Mn)V semiconductors. *Rev. Mod. Phys.* **2006**, *78*, 809–864. [CrossRef]
9. Ohno, H.; Shen, A.; Matsukura, F.; Oiwa, A.; Endo, A.; Katsumoto, S.; Iye, Y. (Ga,Mn)As: A new diluted magnetic semiconductor based on GaAs. *Appl. Phys. Lett.* **1996**, *69*, 363. [CrossRef]
10. Chen, L.; Yang, X.; Yang, F.; Zhao, J.; Misuraca, J.; Xiong, P.; von Molnar, S. Enhancing the Curie temperature of ferromagnetic semiconductor (Ga,Mn)As to 200 K via nanostructure engineering. *Nano Lett.* **2011**, *11*, 2584–2589. [CrossRef]
11. Samarth, N. Ferromagnetic semicondutors: Battle of the bands. *Nat. Mater.* **2012**, *11*, 360–361. [CrossRef]
12. Masek, J.; Kudrnovsky, J.; Maca, F.; Gallagher, B.L.; Campion, R.P.; Gregory, D.H.; Jungwirth, T. Dilute moment n-type ferromagnetic semiconductor Li(Zn,Mn)As. *Phys. Rev. Lett.* **2007**, *98*, 067202. [CrossRef] [PubMed]
13. Deng, Z.; Jin, C.Q.; Liu, Q.Q.; Wang, X.C.; Zhu, J.L.; Feng, S.M.; Chen, L.C.; Yu, R.C.; Arguello, C.; Goko, T.; et al. Li(Zn,Mn)As as a new generation ferromagnet based on a I-II-V semiconductor. *Nat. Commun.* **2011**, *2*, 422. [CrossRef] [PubMed]

14. Deng, Z.; Zhao, K.; Gu, B.; Han, W.; Zhu, J.L.; Wang, X.C.; Li, X.; Liu, Q.Q.; Yu, R.C.; Goko, T.; et al. Diluted ferromagnetic semiconductor Li(Zn,Mn)P with decoupled charge and spin doping. *Phys. Rev. B* **2013**, *88*, 081203. [CrossRef]
15. Ding, C.; Man, H.; Qin, C.; Lu, J.; Sun, Y.; Wang, Q.; Yu, B.; Feng, C.; Goko, T.; Arguello, C.J.; et al. $(La_{1-x}Ba_x)(Zn_{1-x}Mn_x)AsO$: A two-dimensional 1111-type diluted magnetic semiconductor in bulk form. *Phys. Rev. B* **2013**, *88*, 041102. [CrossRef]
16. Ding, C.; Qin, C.; Man, H.Y.; Imai, T.; Ning, F.L. NMR investigation of the diluted magnetic semiconductor $Li(Zn_{1-x}Mn_x)P$ (x=0.1). *Phys. Rev. B* **2013**, *88*, 041108. [CrossRef]
17. Han, W.; Zhao, K.; Wang, X.; Liu, Q.; Ning, F.; Deng, Z.; Liu, Y.; Zhu, J.; Ding, C.; Man, H.; et al. Diluted ferromagnetic semiconductor (LaCa)(ZnMn)SbO isostructural to "1111" type iron pnictide superconductors. *Sci. China Phys. Mech. Astron.* **2013**, *56*, 2026–2030. [CrossRef]
18. Lu, J.; Man, H.; Ding, C.; Wang, Q.; Yu, B.; Guo, S.; Wang, H.; Chen, B.; Han, W.; Jin, C.; et al. The synthesis and characterization of 1111-type diluted magnetic semiconductors $(La_{1-x}Sr_x)(Zn_{1-x}TM_x)AsO$ (TM = Mn, Fe, Co). *Europhys. Lett.* **2013**, *103*, 67011. [CrossRef]
19. Yang, X.; Li, Y.; Shen, C.; Si, B.; Sun, Y.; Tao, Q.; Cao, G.; Xu, Z.; Zhang, F. Sr and Mn co-doped LaCuSO: A wide band gap oxide diluted magnetic semiconductor with Tc around 200 K. *Appl. Phys. Lett.* **2013**, *103*, 022410. [CrossRef]
20. Yang, X.; Li, Y.; Zhang, P.; Jiang, H.; Luo, Y.; Chen, Q.; Feng, C.; Cao, C.; Dai, J.; Tao, Q.; et al. K and Mn co-doped $BaCd_2As_2$: A hexagonal structured bulk diluted magnetic semiconductor with large magnetoresistance. *J. Appl. Phys.* **2013**, *114*, 223905. [CrossRef]
21. Zhao, K.; Deng, Z.; Wang, X.C.; Han, W.; Zhu, J.L.; Li, X.; Liu, Q.Q.; Yu, R.C.; Goko, T.; Frandsen, B.; et al. New diluted ferromagnetic semiconductor with Curie temperature up to 180 K and isostructural to the '122' iron-based superconductors. *Nat. Commun.* **2013**, *4*, 1442. [CrossRef]
22. Chen, B.J.; Zhao, K.; Deng, Z.; Han, W.; Zhu, J.L.; Wang, X.C.; Liu, Q.Q.; Frandsen, B.; Liu, L.; Cheung, S.; et al. $(Sr,Na)(Zn,Mn)_2As_2$: A diluted ferromagnetic semiconductor with the hexagonal $CaAl_2Si_2$ type structure. *Phys. Rev. B* **2014**, *90*, 155202. [CrossRef]
23. Ding, C.; Gong, X.; Man, H.; Zhi, G.; Guo, S.; Zhao, Y.; Wang, H.; Chen, B.; Ning, F.L. The suppression of Curie temperature by Sr doping in diluted ferromagnetic semiconductor $(La_{1-x}Sr_x)(Zn_{1-y}Mn_y)AsO$. *Europhys. Lett.* **2014**, *107*, 17004. [CrossRef]
24. Man, H.; Qin, C.; Ding, C.; Wang, Q.; Gong, X.; Guo, S.; Wang, H.; Chen, B.; Ning, F.L. $(Sr_3La_2O_5)(Zn_{1-x}Mn_x)_2As_2$: A bulk form diluted magnetic semiconductor isostructural to the "32522" Fe-based superconductors. *Europhys. Lett.* **2014**, *105*, 67004. [CrossRef]
25. Ning, F.L.; Man, H.; Gong, X.; Zhi, G.; Guo, S.; Ding, C.; Wang, Q.; Goko, T.; Liu, L.; Frandsen, B.A.; et al. Suppression of *Tc* by overdoped Li in the diluted ferromagnetic semiconductor $Li_{1+y}(Zn_{1-x}Mn_x)P$: A μSR investigation. *Phys. Rev. B* **2014**, *90*, 085123. [CrossRef]
26. Yang, X.; Chen, Q.; Li, Y.; Wang, Z.; Bao, J.; Li, Y.; Tao, Q.; Cao, G.; Xu, Z.-A. $Sr_{0.9}K_{0.1}Zn_{1.8}Mn_{0.2}As_2$: A ferromagnetic semiconductor with colossal magnetoresistance. *EPL (Europhys. Lett.)* **2014**, *107*, 67007. [CrossRef]
27. Zhao, K.; Chen, B.; Zhao, G.; Yuan, Z.; Liu, Q.; Deng, Z.; Zhu, J.; Jin, C. Ferromagnetism at 230 K in $(Ba_{0.7}K_{0.3})(Zn_{0.85}Mn_{0.15})_2As_2$ diluted magnetic semiconductor. *Chin. Sci. Bull.* **2014**, *59*, 2524–2527. [CrossRef]
28. Zhao, K.; Chen, B.J.; Deng, Z.; Han, W.; Zhao, G.Q.; Zhu, J.L.; Liu, Q.Q.; Wang, X.C.; Frandsen, B.; Liu, L.; et al. $(Ca,Na)(Zn,Mn)_2As_2$: A new spin and charge doping decoupled diluted ferromagnetic semiconductor. *J. Appl. Phys.* **2014**, *116*, 163906. [CrossRef]
29. Man, H.; Guo, S.; Sui, Y.; Guo, Y.; Chen, B.; Wang, H.; Ding, C.; Ning, F.L. $Ba(Zn_{1-2x}Mn_xCu_x)_2As_2$: A Bulk Form Diluted Ferromagnetic Semiconductor with Mn and Cu Codoping at Zn Sites. *Sci. Rep.* **2015**, *5*, 15507. [CrossRef]
30. Suzuki, H.; Zhao, G.Q.; Zhao, K.; Chen, B.J.; Horio, M.; Koshiishi, K.; Xu, J.; Kobayashi, M.; Minohara, M.; Sakai, E.; et al. Fermi surfaces and p−d hybridization in the diluted magnetic semiconductor $Ba_{1-x}K_x(Zn_{1-y}Mn_y)_2As_2$ studied by soft x-ray angle-resolved photoemission spectroscopy. *Phys. Rev. B* **2015**, *92*, 235120. [CrossRef]
31. Suzuki, H.; Zhao, K.; Shibata, G.; Takahashi, Y.; Sakamoto, S.; Yoshimatsu, K.; Chen, B.J.; Kumigashira, H.; Chang, F.H.; Lin, H.J.; et al. Photoemission and x-ray absorption studies of the isostructural to Fe-based superconductors diluted magnetic semiconductor $(Ba_{1-x}K_x)(Zn_{1-y}Mn_y)_2As_2$. *Phys. Rev. B* **2015**, *91*, 140401. [CrossRef]
32. Chen, B.; Deng, Z.; Li, W.; Gao, M.; Li, Z.; Zhao, G.; Yu, S.; Wang, X.; Liu, Q.; Jin, C. $(Sr_{1-x}Na_x)(Cd_{1-x}Mn_x)_2As_2$: A new charge and spin doping decoupled diluted magnetic semiconductors with $CaAl_2Si_2$-type structure. *J. Appl. Phys.* **2016**, *120*, 083902. [CrossRef]
33. Chen, B.; Deng, Z.; Li, W.; Gao, M.; Liu, Q.; Gu, C.Z.; Hu, F.X.; Shen, B.G.; Frandsen, B.; Cheung, S.; et al. New Fluoride-arsenide Diluted Magnetic Semiconductor (Ba,K)F(Zn,Mn)As with Independent Spin and Charge Doping. *Sci. Rep.* **2016**, *6*, 36578. [CrossRef]
34. Chen, B.; Deng, Z.; Li, W.; Gao, M.; Zhao, J.; Zhao, G.; Yu, S.; Wang, X.; Liu, Q.; Jin, C. Li(Zn,Co,Mn)As: A bulk form diluted magnetic semiconductor with Co and Mn co-doping at Zn sites. *AIP Adv.* **2016**, *6*, 115014. [CrossRef]

35. Ding, C.; Guo, S.; Zhao, Y.; Man, H.; Fu, L.; Gu, Y.; Wang, Z.; Liu, L.; Frandsen, B.A.; Cheung, S.; et al. The synthesis and characterization of 1111 type diluted ferromagnetic semiconductor $(La_{1-x}Ca_x)(Zn_{1-x}Mn_x)AsO$. *J. Phys. Condens. Matter* **2016**, *28*, 026003. [CrossRef]
36. Frandsen, B.A.; Gong, Z.; Terban, M.W.; Banerjee, S.; Chen, B.; Jin, C.; Feygenson, M.; Uemura, Y.J.; Billinge, S.J.L. Local atomic and magnetic structure of dilute magnetic semiconductor$(Ba,K)(Zn,Mn)_2As_2$. *Phys. Rev. B* **2016**, *94*, 094102. [CrossRef]
37. Guo, S.; Man, H.; Gong, X.; Ding, C.; Zhao, Y.; Chen, B.; Guo, Y.; Wang, H.; Ning, F.L. $(Ba_{1-x}K_x)(Cu_{2-x}Mn_x)Se_2$: A copper-based bulk form diluted magnetic semiconductor with orthorhombic $BaCu_2S_2$-type structure. *J. Magn. Magn. Mater.* **2016**, *400*, 295–299. [CrossRef]
38. Guo, S.; Zhao, Y.; Gong, X.; Man, H.; Ding, C.; Zhi, G.; Fu, L.; Gu, Y.; Wang, H.; Chen, B.; et al. $La(Zn_{1-2x}Mn_xCu_x)AsO$: A 1111-type diluted magnetic semiconductor with manganese and copper codoping at Zn sites. *Europhys. Lett.* **2016**, *114*, 57008. [CrossRef]
39. Guo, S.L.; Zhao, Y.; Man, H.Y.; Ding, C.; Gong, X.; Zhi, G.X.; Fu, L.C.; Gu, Y.L.; Frandsen, B.A.; Liu, L.; et al. μSR investigation of a new diluted magnetic semiconductor Li(Zn,Mn,Cu)As with Mn and Cu codoping at the same Zn sites. *J. Phys. Condens. Matter* **2016**, *28*, 366001. [CrossRef]
40. Sun, F.; Li, N.N.; Chen, B.J.; Jia, Y.T.; Zhang, L.J.; Li, W.M.; Zhao, G.Q.; Xing, L.Y.; Fabbris, G.; Wang, Y.G.; et al. Pressure effect on the magnetism of the diluted magnetic semiconductor $(Ba_{1-x}K_x)(Zn_{1-y}Mn_y)_2As_2$ with independent spin and charge doping. *Phys. Rev. B* **2016**, *93*, 224403. [CrossRef]
41. Sun, F.; Xu, C.; Yu, S.; Chen, B.-J.; Zhao, G.-Q.; Deng, Z.; Yang, W.-G.; Jin, C.-Q. Synchrotron X-Ray Diffraction Studies on the New Generation Ferromagnetic Semiconductor Li(Zn,Mn)As under High Pressure. *Chin. Phys. Lett.* **2017**, *34*, 067501. [CrossRef]
42. Sun, F.; Zhao, G.Q.; Escanhoela, C.A.; Chen, B.J.; Kou, R.H.; Wang, Y.G.; Xiao, Y.M.; Chow, P.; Mao, H.K.; Haskel, D.; et al. Hole doping and pressure effects on the II-II-V-based diluted magnetic semiconductor $(Ba_{1-x}K_x)(Zn_{1-y}Mn_y)_2As_2$. *Phys. Rev. B* **2017**, *95*, 094412. [CrossRef]
43. Wang, R.; Huang, Z.X.; Zhao, G.Q.; Yu, S.; Deng, Z.; Jin, C.Q.; Jia, Q.J.; Chen, Y.; Yang, T.Y.; Jiang, X.M.; et al. Out-of-plane easy-axis in thin films of diluted magnetic semiconductor $Ba_{1-x}K_x(Zn_{1-y}Mn_y)_2As_2$. *AIP Adv.* **2017**, *7*, 045017. [CrossRef]
44. Zhao, G.Q.; Zhao, G.Q.; Lin, C.J.; Deng, Z.; Gu, G.X.; Yu, S.; Wang, X.C.; Gong, Z.Z.; Uemura, Y.J.; Li, Y.Q.; et al. Single Crystal Growth and Spin Polarization Measurements of Diluted Magnetic Semiconductor $(BaK)(ZnMn)_2As_2$. *Sci. Rep.* **2017**, *7*, 14473. [CrossRef]
45. Zhao, Y.; Wang, K.; Guo, S.; Fu, L.; Gu, Y.; Zhi, G.; Xu, L.; Cui, Q.; Cheng, J.; Wang, H.; et al. $La(Zn_{1-2x}Mn_xCu_x)SbO$: A new diluted magnetic semiconductor isostructural to 1111-type iron pnictide superconductors. *EPL (Europhys. Lett.)* **2017**, *120*, 47005. [CrossRef]
46. Surmach, M.A.; Chen, B.J.; Deng, Z.; Jin, C.Q.; Glasbrenner, J.K.; Mazin, I.I.; Ivanov, A.; Inosov, D.S. Weak doping dependence of the antiferromagnetic coupling between nearest-neighbor $Mn^{2+}$ spins in $(Ba_{1-x}K_x)(Zn_{1-y}Mn_y)_2As_2$. *Phys. Rev. B* **2018**, *97*, 104418. [CrossRef]
47. Zhao, G.Q.; Li, Z.; Sun, F.; Yuan, Z.; Chen, B.J.; Yu, S.; Peng, Y.; Deng, Z.; Wang, X.C.; Jin, C.Q. Effects of high pressure on the ferromagnetism and in-plane electrical transport of $(Ba_{0.904}K_{0.096})(Zn_{0.805}Mn_{0.195})_2As_2$ single crystal. *J. Phys. Condens. Matter* **2018**, *30*, 254001. [CrossRef] [PubMed]
48. Fu, L.; Gu, Y.; Guo, S.; Wang, K.; Zhang, H.; Zhi, G.; Liu, H.; Xu, Y.; Wang, Y.; Wang, H.; et al. Ferromagnetism in fluoride-antimonide $SrF(Zn_{1-2x}Mn_xCu_x)Sb$ with a quasi two dimensional structure. *J. Magn. Magn. Mater.* **2019**, *483*, 95–99. [CrossRef]
49. Han, W.; Chen, B.J.; Gu, B.; Zhao, G.Q.; Yu, S.; Wang, X.C.; Liu, Q.Q.; Deng, Z.; Li, W.M.; Zhao, J.F.; et al. Li(Cd,Mn)P: A new cadmium based diluted ferromagnetic semiconductor with independent spin & charge doping. *Sci. Rep.* **2019**, *9*, 7490.
50. Peng, Y.; Yu, S.; Zhao, G.Q.; Li, W.M.; Zhao, J.F.; Cao, L.P.; Wang, X.C.; Liu, Q.Q.; Zhang, S.J.; Yu, R.Z.; et al. Effects of chemical pressure on diluted magnetic semiconductor $(Ba,K)(Zn,Mn)_2As_2$. *Chin. Phys. B* **2019**, *28*, 057501. [CrossRef]
51. Yu, S.; Zhao, G.; Peng, Y.; Zhu, X.; Wang, X.; Zhao, J.; Cao, L.; Li, W.; Li, Z.; Deng, Z.; et al. A substantial increase of Curie temperature in a new type of diluted magnetic semiconductors via effects of chemical pressure. *APL Mater.* **2019**, *7*, 10. [CrossRef]
52. Gu, Y.; Zhang, H.; Zhang, R.; Fu, L.; Wang, K.; Zhi, G.; Guo, S.; Ning, F.L. A novel diluted magnetic semiconductor $(Ca,Na)(Zn,Mn)_2Sb_2$ with decoupled charge and spin dopings. *Chin. Phys. B* **2020**, *29*, 057507. [CrossRef]
53. Shen, X.; Deng, Z.; Li, Z.; Gu, B.; He, L.H.; Yao, Y.; Jin, C.Q.; Yu, R.C. Effects of structure modulation on the magnetic properties in diluted magnetic semiconductor $Li_{1+y}Zn_{0.9}Mn_{0.1}As_{1.0}$. *Phys. Rev. Mater.* **2020**, *4*, 094412. [CrossRef]
54. Yu, S.; Liu, X.; Zhao, G.; Peng, Y.; Wang, X.; Zhao, J.; Li, W.; Deng, Z.; Furdyna, J.K.; Uemura, Y.J.; et al. Anomalous critical point behavior in dilute magnetic semiconductor $(Ca,Na)(Zn,Mn)_2Sb_2$. *Phys. Rev. Mater.* **2020**, *4*, 024411. [CrossRef]
55. Yu, S.; Zhao, G.; Peng, Y.; Wang, X.; Liu, Q.; Yu, R.; Zhang, S.; Zhao, J.; Li, W.; Deng, Z.; et al. $(Ba,K)(Zn,Mn)_2Sb_2$: A New Type of Diluted Magnetic Semiconductor. *Crystals* **2020**, *10*, 690. [CrossRef]
56. Sakamoto, S.; Zhao, G.Q.; Shibata, G.; Deng, Z.; Zhao, K.; Wang, X.C.; Nonaka, Y.; Ikeda, K.; Chi, Z.D.; Wan, Y.X.; et al. Anisotropic Spin Distribution and Perpendicular Magnetic Anisotropy in a Layered Ferromagnetic Semiconductor $(Ba,K)(Zn,Mn)_2As_2$. *ACS Appl. Electron. Mater.* **2021**, *3*, 789–794. [CrossRef]

57. Zhang, H.J.; Zhang, R.F.; Fu, L.C.; Gu, Y.L.; Zhi, G.X.; Dong, J.O.; Zhao, X.Q.; Ning, F.L. $(La_{1-x}Sr_x)(Zn_{1-x}Mn_x)SbO$: A novel 1111-type diluted magnetic semiconductor. *Acta Physica. Sinica.* **2021**, *70*, 107501. [CrossRef]
58. Zhi, G.; Guo, S.; Zhang, R.; Zhao, Y.; Fu, L.; Gu, Y.; Wang, K.; Zhang, H.; Zhao, X.; Dong, J.; et al. $Cu_2(Zn,Mn)(Sn,Al)Se_4$: A diluted magnetic semiconductor with decoupled charge and spin doping. *J. Magn. Magn. Mater.* **2021**, *536*, 168064. [CrossRef]
59. Dong, J.; Zhao, X.; Fu, L.; Gu, Y.; Zhang, R.; Yang, Q.; Xie, L.; Ning, F. $(Ca,K)(Zn,Mn)_2As_2$: Ferromagnetic semiconductor induced by decoupled charge and spin doping in $CaZn_2As_2$. *J. Semicond.* **2022**, *43*, 072501. [CrossRef]
60. Gu, Y.; Zhang, R.; Zhang, H.; Fu, L.; Zhi, G.; Dong, J.; Zhao, X.; Xie, L.; Ning, F. A $CaAl_2Si_2$-Type Magnetic Semiconductor $(Sr,Na)(Zn,Mn)_2Sb_2$ Isostructural to 122-Type Iron-Based Superconductors. *Adv. Condens. Matter Phys.* **2022**, *2022*, 4291923. [CrossRef]
61. Suzuki, H.; Zhao, G.; Okamoto, J.; Sakamoto, S.; Chen, Z.-Y.; Nonaka, Y.; Shibata, G.; Zhao, K.; Chen, B.; Wu, W.-B.; et al. Magnetic Properties and Electronic Configurations of Mn Ions in the Diluted Magnetic Semiconductor $Ba_{1-x}K_x(Zn_{1-y}Mn_y)_2As_2$ Studied by X-ray Magnetic Circular Dichroism and Resonant Inelastic X-ray Scattering. *J. Phys. Soc. Jpn.* **2022**, *91*, 064710. [CrossRef]
62. Zhang, R.; Xu, C.; Fu, L.; Gu, Y.; Zhi, G.; Dong, J.; Zhao, X.; Xie, L.; Zhang, H.; Cao, C.; et al. Manipulation of the ferromagnetic ordering in magnetic semiconductor (La,Ca)(Zn,Mn)AsO by chemical pressure. *J. Magn. Magn. Mater.* **2022**, *554*, 169276. [CrossRef]
63. Zhao, X.; Dong, J.; Fu, L.; Gu, Y.; Zhang, R.; Yang, Q.; Xie, L.; Tang, Y.; Ning, F. $(Ba_{1-x}Na_x)F(Zn_{1-x}Mn_x)Sb$: A novel fluoride-antimonide magnetic semiconductor with decoupled charge and spin doping. *J. Semicond.* **2022**, *43*, 112501. [CrossRef]
64. Yu, S.; Peng, Y.; Zhao, G.; Zhao, J.; Wang, X.; Zhang, J.; Deng, Z.; Jin, C.Q. Colossal negative magnetoresistance in spin glass Na(Zn,Mn)Sb. *J. Semicond.* **2023**, *44*, 032501. [CrossRef]
65. Peng, Y.; Li, X.; Shi, L.; Zhao, G.; Zhang, J.; Zhao, J.; Wang, X.; Gu, B.; Deng, Z.; Uemura, Y.J.; et al. A Near Room Temperature Curie Temperature in a New Type of Diluted Magnetic Semiconductor $(Ba,K)(Zn,Mn)_2As_2$. *Adv. Phys. Res.* **2025**, *4*, 2400124. [CrossRef]
66. Peng, Y.; Peng, Y.; Shi, L.; Zhao, G.; Zhang, J.; Zhao, J.; Wang, X.; Deng, Z.; Jin, C.Q. Colossal Magnetoresistance in Layered Diluted Magnetic Semiconductor $Rb(Zn,Li,Mn)_4As_3$ Single Crystals. *Nanomaterials* **2024**, *14*, 263. [CrossRef]
67. Zhao, G.Q.; Bo, G.; Kojima, K.M.; Cai, Y.P.; Li, X.; Peng, Y.; Zhao, K.; Guo, S.L.; Han, W.; Yongqing Li, Y.Q.; et al. Doping effects on magnetic evolution and transport properties in $(Ba,Rb)(Zn,Mn)_2As_2$. *Nanomaterials*. *under review*.
68. Hirohata, A.; Sukegawa, H.; Yanagihara, H.; Zutic, I.; Seki, T.; Mizukami, S.; Swaminathan, R. Roadmap for Emerging Materials for Spintronic Device Applications. *IEEE Trans. Magn.* **2015**, *51*, 0800511. [CrossRef]
69. Eggenkamp, P.J.T.; Swagten, H.J.M.; Story, T.; Litvinov, V.I.; Swuste, C.H.W.; Dejonge, W.J.M. Calculations of the ferromagnet-to-spin-glass transition in diluted magnetic systems with an RKKY interaction. *Phys. Rev. B* **1995**, *51*, 15250–15259. [CrossRef]
70. Ferrand, D.; Cibert, J.; Wasiela, A.; Bourgognon, C.; Tatarenko, S.; Fishman, G.; Andrearczyk, T.; Jaroszyński, J.; Koleśnik, S.; Dietl, T.; et al. Carrier-induced ferromagnetism in $p-Zn_{1-x}Mn_xTe$. *Phys. Rev. B* **2001**, *63*, 085201. [CrossRef]
71. Topping, C.V.; Blundell, S.J.A.C. susceptibility as a probe of low-frequency magnetic dynamics. *J. Phys. Condens. Matter* **2019**, *31*, 013001. [CrossRef] [PubMed]
72. Yaouanc, A.; de Réotier, P.D.; Rotation, M.S. *Relaxation, and Resonance: Applications to Condensed Matter*; Oxford University Press: Oxford, UK, 2010.
73. Amato, A.; Morenzoni, E. *Introduction to Muon Spin Spectroscopy: Applications to Solid State and Material Sciences*; Springer: Berlin/Heidelberg, Germany, 2024.
74. Blundell, S.J. Spin-polarized muons in condensed matter physics. *Contemp. Phys.* **1999**, *40*, 175–192. [CrossRef]
75. Uemura, Y.J.; Yamazaki, T.; Harshman, D.R.; Senba, M.; Ansaldo, E.J. Muon-spin relaxation in AuFe and CuMn spin glasses. *Phys. Rev. B* **1985**, *31*, 546–563. [CrossRef] [PubMed]
76. Balz, C.; Lake, B.; Reuther, J.; Luetkens, H.; Schönemann, R.; Herrmannsdörfer, T.; Singh, Y.; Nazmul Islam, A.T.M.; Wheeler, E.M.; Rodriguez-Rivera, J.A.; et al. Physical realization of a quantum spin liquid based on a complex frustration mechanism. *Nat. Phys.* **2016**, *12*, 942–949. [CrossRef]
77. Coey, J.M.D. *Magnetism and Magnetic Materials*; Cambridge University Press: Cambridge, UK, 2010.
78. Coey, J.M.D.; Freitas, P.P.; Plaskett, T.S.; von Molnar, S. Giant transverse hysteresis in an asperomagnet. *Phys. Rev. B* **1990**, *41*, 9585–9587. [CrossRef]
79. Tissier, B.; Buder, R.; Coey, J.M.D. Domains in an asperomagnet: Amorphous DyCu. *J. Magn. Magn. Mater.* **1980**, *15*, 1393–1394. [CrossRef]